Journal of Thermal Analysis and Calorimetry, Vol. 92 (2008) 2, 607–616

SYNTHESIS, CHARACTERIZATION AND THERMAL DECOMPOSITION OF Sb^{III}–M–Sb^{III} TYPE TRINUCLEAR COMPLEXES OF ETHYLENEDIAMINE-N, N, N’, N’- TETRAACETATE (*M*:Co(II), La(III), Nd(III), Dy(III))

G. Q. Zhong[1*], *J. Shen*[1], *Q. Y. Jiang*[1], *Y. Q. Jia*[2], *M. J. Chen*[1] *and Z. P. Zhang*[1]

[1]Department of Chemistry, Southwest University of Science and Technology, Mianyang 621010, China
[2]Department of Chemistry, East China University of Science and Technology, Shanghai 200237, China

Four ethylenediamine-N,N,N’,N’-tetraacetate complexes with Sb(III)–M–Sb(III) polynuclear structure (*M*=Co(II), La(III), Nd(III), Dy(III)) are synthesized. $[Sb_2\text{-}\mu_4\text{-}(EDTA)_2Co(H_2O)_2]\cdot 5.15H_2O$ is characterized by single crystal X-ray diffraction. The crystal structure of $[Sb_2\text{-}\mu_4\text{-}(EDTA)_2Co(H_2O)_2]\cdot 5.15H_2O$ belongs to monoclinic system, space group $P2_1/n$, lattice parameters: a=6.9969(2), b=20.8705(4), c=10.8106(2) Å, β=90.031(1)°, V=1578.66(6) Å^3, Z=2, M_r=1007.76, D_c=2.120 g cm^{-3}, $F(000)$=1001, μ=2.323 mm^{-1}, the final R=0.0235 and wR=0.0629 for 3480 observed reflections ($I>2\sigma(I)$). The powder X-ray diffraction patterns of the complexes are also measured. Elemental analyses, FTIR spectra, TG-DSC and DTA of $[Sb_2(EDTA)_2Ln]NO_3\cdot nH_2O$ are performed. FTIR spectra reveal that the antimony and other metallic ions were connected through the carboxylate bridges. The thermal analysis can demonstrate the complex formation of the antimony, other metallic ions and EDTA. The possible pyrolysis reactions in the thermal decomposition process of the complexes, the experimental and calculated percentage mass losses are also given.

Keywords: *antimony, complex, crystal structure, rare earth metal, thermal decomposition*

Introduction

There has been much interest in the coordination chemistry of ethylenediamine-N,N,N’,N’-tetraacetate (EDTA) in recent decades, because EDTA can act as a multi-dentate ligand linking transition metal ions and main group metal ions. Investigations for the synthesis and structures of various bimetallic EDTA complexes have always attracted the attention of chemists in view of their fascinating structural diversity and potential properties. Some complexes with lanthanide and transition metals have been isolated and structurally characterized [1–4]. For instance, $Ln_2M_3(EDTA)_3(H_2O)_{11}\cdot 12H_2O$ (*Ln*=Nd, Gd; *M*=Mn, Co), $[LnCuCl(NTA)(H_2O)_6]ClO_4\cdot H_2O$ (*Ln*=La, Ce, Pr, Gd, Tb and Dy) [5] and $[LnCuCl(NTA)(H_2O)_6]\cdot ClO_4\cdot 3H_2O$ (*Ln*=Ho, Er, Tm, Lu and Y), and the magnetic properties of lanthanide(Ln)-transition metal coordination polymers were studied [4]. Some complexes of the antimony and lanthanide possess a certain biologic or medicinal function [6]. Therefore, to synthesize the new complexes of the antimony ion, lanthanide ion and various organic ligands is very interesting not only for coordination chemistry, but also for the pharmaceutical chemistry.

In this paper, we shall give the synthesis process of new EDTA-linked heteronuclear antimony complexes, the results of the powder X-ray diffraction and the infrared spectra of the complexes. In recent years, some papers about the thermal analysis of the polynuclear complexes are published [7–9]. So, we shall also report the results of thermal decomposition of the new complexes and give some analytical results for the intermediate and the final residues in the thermal decomposition process to check the pyrolysis reaction of the complexes. As part of a study of the relation between the structure and properties, the synthesis process and the single crystal structure of the analogous complex $[Sb_2\text{-}\mu_4\text{-}(EDTA)_2Co(H_2O)_2]\cdot 5.15H_2O$ are also given.

Experimental

All chemicals are reagent grade as received from commercial sources and without further purification. $Ln(NO_3)_3\cdot 6H_2O$ (*Ln*=La, Nd and Dy) were prepared by dissolving the corresponding oxides (99.9%) in 1:1 nitric acid, respectively, and concentrating the solution. Preparation of each complex was carried out through 2 stages. Stage 1: Preparation of

---

[*] Author for correspondence: zgq316@163.com

1388–6150/$20.00

Akadémiai Kiadó, Budapest, Hungary
Springer, Dordrecht, The Netherlands

Table 1 Elemental analysis results of the complexes

Complex	Composition	Calcd./%					Found/%				
		C	H	N	Sb	Ln	C	H	N	Sb	Ln
H[Sb(EDTA)]·H_2O	$C_{10}H_{15}O_9N_2Sb$	27.78	3.46	6.42	28.23	–	28.00	3.52	6.53	28.38	–
[Sb_2(EDTA)$_2$La]NO_3·8H_2O	$C_{20}H_{40}N_5O_{27}LaSb_2$	20.67	3.099	5.760	20.72	11.97	20.62	3.46	6.01	20.90	11.92
[Sb_2(EDTA)$_2$Nd]NO_3·7H_2O	$C_{20}H_{38}N_5O_{26}NdSb_2$	21.91	3.145	6.079	21.12	12.85	20.85	3.32	6.08	21.13	12.52
[Sb_2(EDTA)$_2$Dy]NO_3·7H_2O	$C_{20}H_{38}N_5O_{26}DySb_2$	20.78	3.083	5.818	20.66	14.01	20.52	3.27	5.98	20.80	13.88

H[Sb(EDTA)]·H_2O. 5 mmol H_4EDTA was dissolved in 100 mL hot distilled water, then, 3 mmol antimonous oxide is added to the above mentioned solution. After stirring the solution for 6 h at 95°C, the solution was filtered while hot. The clear and colorless filtrate was concentrated. When slowly cooling the filtate, the small crystals were obtained. Stage 2(A): Preparation of the Sb(III)–Co(II) heteronuclear complex. 1 mmol of H[Sb(EDTA)]·H_2O prepared in stage 1 was dissolved in 50 mL hot distilled water and the solution was heated to 95°C. Then, the superfluous cobalt carbonate basic was gradually added to the above solution. Stirring the solution for 2 days at 95°C, most solids were dissolved. The resultant solution was purple. After cooling the solution to room temperature, the solution is filtered and concentrated. The concentrated solution held about 2 weeks. The crystals were obtained as purple thin plates. The yield is about 84%. After recrystallizing, the single crystals can be obtained as pink thin block. The yield is about 76%. Stage 2(B): Preparation of the Sb–Ln heteronuclear complex. 1 mmol of H[Sb(EDTA)]·H_2O prepared in stage 1 was dissolved in 50 mL hot distilled water and the solution was heated to 95°C. Then, gradually adding 1 mmol NH_4HCO_3 to the solution and stirring the solution for 30 min. After cooling the solution to room temperature, to mix the above solution and 1 mmol $Ln(NO_3)_3 \cdot 6H_2O$ (*Ln*=La, Nd and Dy), in this case, the transparent solution was obtained. The mixture solution held for a week. The block crystals were isolated from the solution.

The content of carbon, hydrogen and nitrogen in the crystals were determined by vario EL III elemental analyzer. Antimony and lanthanide were measured by classical semimicro quantitative methods. First, the samples were heated in the furnace at 800°C for 4 h. To dissolve the sample by a small quantity of diluted hydrochloric acid, Antimony in the sample solution was determined by iodimetry. To add 20% Seignette salt to the sample solution as screening agent for antimony, then, lanthanide in the sample solution was measured by EDTA titration. The elemental analysis results are listed in Table 1.

For $[Sb_2\text{-}\mu_4\text{-}(EDTA)_2Co(H_2O)_2]\cdot 5.15H_2O$ single crystal, a suitable pink block crystal with approximate dimensions of 0.43×0.20×0.17 mm was carefully selected was mounted on a glass fiber and scanned on a Rigaku RAXIS-RAPID diffractometer at 153(2) K using a graphite-monochromator MoK_α radiation (λ=0.71073 Å) and ω scans technique in the range of $3.07<\theta<27.48°$. The 15295 reflections were measured, of which 3603 (R_{int}=0.0309) were unique. The structure was solved by a direct method through SHELXS-97 program and refined with SHELXL-97 [9, 10] by full-matrix least-squares techniques on F^2. All non-hydrogen atoms were refined anisotropically and the H atoms were located geometrically and refined isotropically. Structure solution and refinement based on 3480 observed with $I>2\sigma(I)$ gave the final R=0.0235, wR=0.0629, S=1.001 and $(\Delta/\sigma)_{\max}$=0.001. The highest and lowest residual peaks in the final difference Fourier map are 0.783 and –1.237 e Å^{-3}, respectively. The molecular structure of $[Sb_2\text{-}\mu_4\text{-}(EDTA)_2Co(H_2O)_2]\cdot 5.15H_2O$ is shown in Fig. 1.

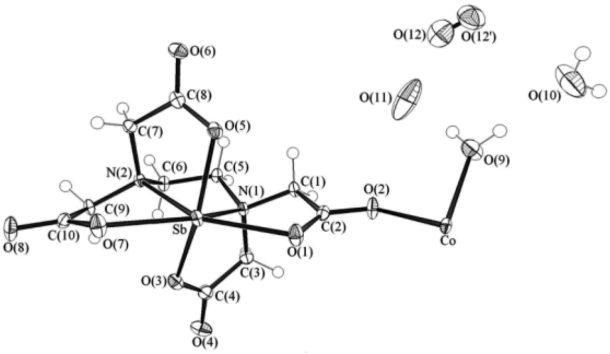

Fig. 1 A view of the molecular asymmetry unit of compound $[Sb_2\text{-}\mu_4\text{-}(EDTA)_2Co(H_2O)_2]\cdot 5.15H_2O$, showing the atom-numbering scheme

The powder X-ray diffraction patterns of the samples were recorded by a D/max-YB X-ray diffractometer, CuK_{α_1} radiation, at room temperature. The powder X-ray diffraction patterns are shown in Fig. 2. Infrared absorption spectra of the samples were recorded in the range 4000–200 cm^{-1} using a Nicolet 570 spectrometer, KBr plate. FTIR spectra are shown in Fig. 3. Thermal studies for the samples were performed by a STA 449C thermal analyzer, in the air, a heating rate of 10°C min^{-1}, the reference α-Al_2O_3. TG-DSC curves are shown in Fig. 4. DTA curves of the samples were obtained on a WCR-1B made in China, in the air, a heating rate of 10°C min^{-1}, the reference α-Al_2O_3. DTA curves are shown in Fig. 5. The possible thermal decomposition process, the experimental and calculated results for the thermal analysis of the samples is summarized in Table 2.

Results and discussion

As the molecular asymmetry unit of compound $[Sb_2\text{-}\mu_4\text{-}(EDTA)_2Co(H_2O)_2]\cdot 5.15H_2O$ in Fig. 1 shows, EDTA is coordinated to Sb(III) and Co(II) ions. The Sb(III) ion is coordinated to four O atoms and two N atoms from EDTA. The coordination number of Co atom is six and its coordination environment is composed of four carboxylic oxygen atoms from four dif-

Table 2 Thermal decomposition data of $[Sb_2\text{-}\mu_4\text{-}(EDTA)_2Co(H_2O)_2]\cdot5.15H_2O$, $[Sb_2(EDTA)_2La]NO_3\cdot8H_2O$, $[Sb_2(EDTA)_2Nd]NO_3\cdot9H_2O$ and $[Sb_2(EDTA)_2Dy(H_2O)_4]NO_3\cdot3H_2O$

Reaction	T/°C	Mass loss/%	
		$W_{exp.}$	$W_{theor.}$
$[Sb_2\text{-}\mu_4\text{-}(EDTA)_2Co(H_2O)_2]\cdot5.15H_2O$			
$\downarrow -7.15H_2O$	130.0 (endo.)	13.10	12.77
$[Sb_2\text{-}\mu_4\text{-}(EDTA)_2Co]$			
$\downarrow -2(CH_2)_2NCH_2COO$			
$\downarrow -2N(CH_2)_3$	357.2 (exo.)	32.59	30.96
$(CoSb_2O_6)(CO)_6$			
$\downarrow -6CO$	527.5 (exo.)	15.92	16.67
$CoSb_2O_6$		38.39*	39.54**
$2[Sb_2(EDTA)_2La]NO_3\cdot8H_2O$			
$\downarrow -16H_2O$	123.6 (endo.)	12.99	12.37
$2[Sb_2(EDTA)_2La]NO_3$			
$\downarrow -2NO_2, -O_2$			
$\downarrow -4(CH_2)_2NCH_2COO$	329.2 (exo.)	21.49	22.51
$2\{^{2+}Sb–Sb^{2+}\}2\{[N(CH_2COO)_3^{3-}]_2\}\{^{2+}La–La^{2+}\}$			
$\downarrow -4N(CH_2)_3$			
$\downarrow -2CO_2$	368.4 (exo.)	12.85	13.41
$\{2[Sb_2O_3]\}\{10[CO]\}\{OLaO–OLaO\}$			
$\downarrow -10CO$			
$\downarrow -0.5O_2$	489.6 (exo.)	11.64	12.71
$2Sb_2O_3+La_2O_3$		41.03*	39.01**
$2[Sb_2(EDTA)_2Nd]NO_3\cdot7H_2O$			
$\downarrow -14H_2O$	120.7 (endo.)	10.54	10.93
$2[Sb_2(EDTA)_2Nd]NO_3$			
$\downarrow -2NO_2, -O_2$			
$\downarrow -4(CH_2)_2NCH2COO$	343.6 (exo.)	22.37	22.72
$2\{^{2+}Sb–Sb^{2+}\}_2\{[N(CH_2COO)_3^{3-}]_2\}\{^{2+}Nd–Nd^{2+}\}$			
$\downarrow -4N(CH_2)_3$			
$\downarrow -6CO$	391.0 (endo.)	17.57	17.03
$\{2[OSbO–OSbO]\}\{6[CO]\}\{ONdO–ONdO\}$			
$\downarrow -6CO$			
$\downarrow -1.5O_2$	464.5 (exo.)	10.65	9.38
$2Sb_2O_3+Nd_2O_3$		38.87*	39.99**
$2[Sb_2(EDTA)_2Dy(H_2O)_4]NO_3\cdot3H_2O$			
$\downarrow -6H_2O$	114.5 (endo.)	5.00	4.62
$\downarrow -8H_2O$	138.2 (endo.)	5.25	6.16
$2[Sb_2(EDTA)_2Dy]NO_3$			
$\downarrow -2NO_2, -O_2$	350.2 (exo.)	22.42	22.40
$\downarrow -4(CH_2)_2NCH_2COO$			
$2\{^{2+}Sb–Sb^{2+}\}2\{[N(CH_2COO)_3^{3-}]_2\}\{^{2+}Dy–Dy^{2+}\}$			
$\downarrow -4N(CH_2)_3$	378.5(exo.)	16.71	16.76
$\downarrow -6CO$			
$\{2[OSbO–OSbO]\}\{6[CO]\}\{ODyO–ODyO\}$			
$\downarrow -6CO$	479.8 (exo.)	8.90	9.23
$\downarrow -1.5O_2$		41.72*	40.84**
$2Sb_2O_3+Dy_2O_3$			

*The calculated mass% of the residue in the sample

**the experimental mass% of the residue in the sample

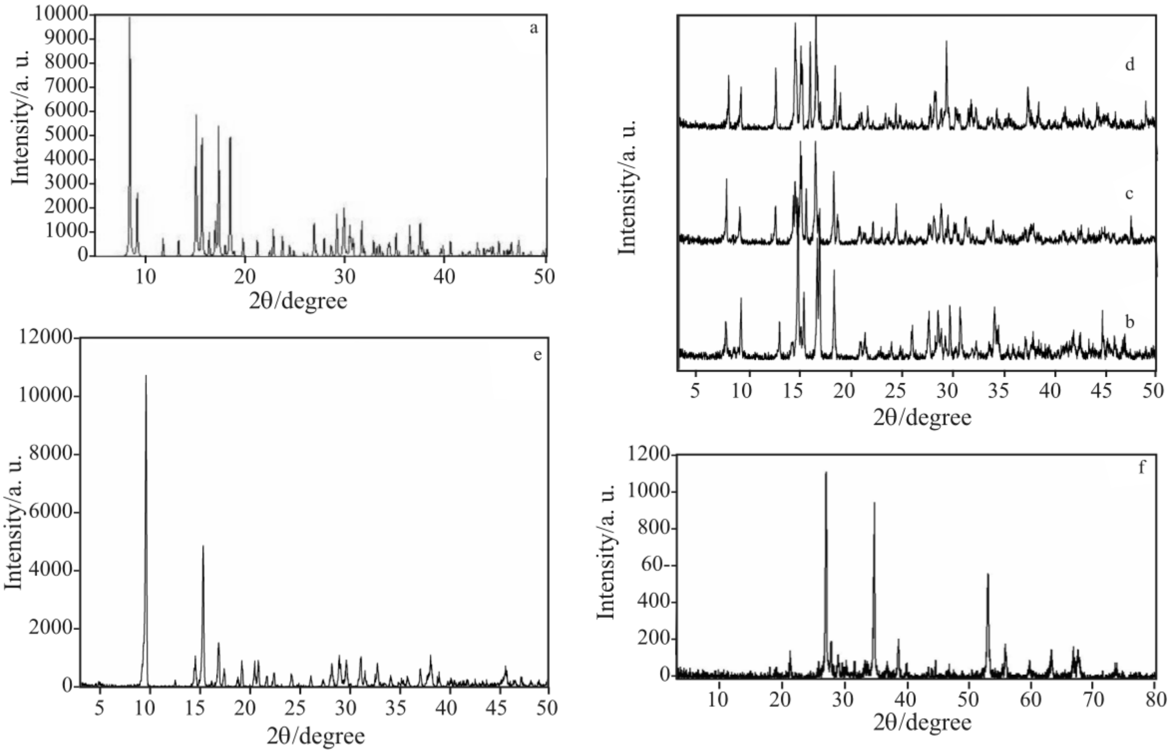

Fig. 2 X-ray powder spectra of a – $[Sb_2\text{-}\mu_4\text{-}(EDTA)_2Co(H_2O)_2]\cdot5.15H_2O$, b – $[Sb_2(EDTA)_2La]NO_3\cdot8H_2O$, c – $[Sb_2(EDTA)_2Nd]NO_3\cdot7H_2O$, d – $[Sb_2(EDTA)_2Dy(H_2O)_4]NO_3\cdot3H_2O$, e – $H[Sb(EDTA)]\cdot H_2O$ and f – $CoSb_2O_6$

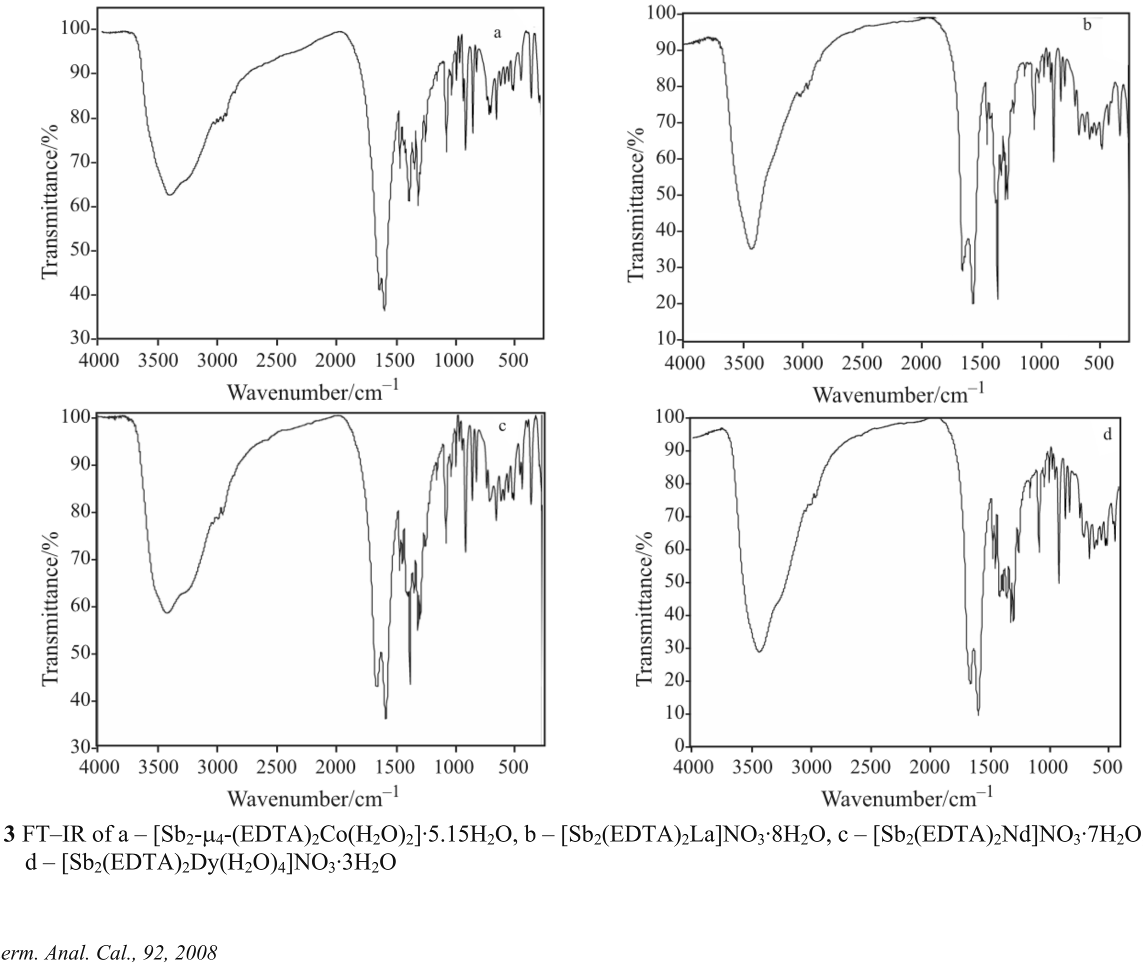

Fig. 3 FT–IR of a – $[Sb_2\text{-}\mu_4\text{-}(EDTA)_2Co(H_2O)_2]\cdot5.15H_2O$, b – $[Sb_2(EDTA)_2La]NO_3\cdot8H_2O$, c – $[Sb_2(EDTA)_2Nd]NO_3\cdot7H_2O$, d – $[Sb_2(EDTA)_2Dy(H_2O)_4]NO_3\cdot3H_2O$

ferent EDTA and two oxygen atoms from two H_2O molecules. The bridging modes of the carboxyl are bidentate, one carboxylic O(1) or O(7) atom is coordinated to Sb(II) and the O(2) or O(8) atom is coordinated to Co(II), as well as, two O atoms (O(4) and O(6)) are unbound.

The powder X-ray diffraction pattern of the Sb–Co complex is almost identical with respect to the positions and intensities of the diffraction peaks for the Sb–Ln complex, as shown in Figs 2a–d. But, the powder X-ray diffraction patterns of these complexes are different from that of $H[Sb(EDTA)]\cdot H_2O$, as shown in Fig. 2e. Obviously, the complexes must be new EDTA-linked heteronuclear ones.

As Fig. 3a shows, the infrared spectra of $[Sb_2\text{-}\mu_4\text{-}(EDTA)_2Co(H_2O)_2]\cdot 5.15H_2O$ makes out a broad peak at 3403 cm^{-1} due to ν_{OH} vibrations of the water molecule. The frequency of the peak is higher than 3400 cm^{-1} showing that the O atoms of the water molecule are coordinated to the metal ions [12]. The absorption peaks at 1602, 1425 and 1395 cm^{-1} may be from the asymmetric and symmetric stretching vibration in the carboxyl groups, respectively. The differences (1602–1425=177 and 1602–1395=207 cm^{-1}) between the frequencies of the asymmetric and symmetric stretching vibration confirms that the oxygen atoms of bridge carboxylic groups are coordinated to Sb(III) and Co(II) ions [13–15]. It can be expected that there must also be the corresponding peaks at 710 and 627 cm^{-1} from the different deformation vibration in the carboxyl groups [16]. It is found that the $\nu_{as(COO)}$ at 1690 cm^{-1} of EDTA red-shifts to 1602 cm^{-1} (non-bridge carboxylic groups) in the complex and $\nu_{s(COO)}$ at 1353 cm^{-1} of EDTA blue-shifts to 1395 cm^{-1} (bridge carboxylic groups) and 1425 cm^{-1} (non-bridge carboxylic groups) in the complex. This means that the O atoms of carboxylic groups coordinate with Sb(III) and Co(II) ions [13–15]. The absorption peaks at 1080 and 1038 cm^{-1} may be from various stretching vibrations of the C–N and C–C bond in EDTA, respectively. In the far-infrared region, the frequency of the stretching vibration of the Sb–N and Sb–O bond is 457 and 371 cm^{-1}, respectively [12, 17]. It may be reasonable to assign the peaks at 592 cm^{-1} to the stretching vibration of Co–O bond in the complex [17, 18]. As Figs 3b–d show, the infrared spectra of $[Sb_2(EDTA)_2Ln]NO_3\cdot nH_2O$ (*Ln*=La, Nd and Dy; *n*=8 or 7) also show a broad peak at 3419, 3420, 3423 cm^{-1}, respectively, due to ν_{OH} vibrations of the water molecules. The frequencies of the peaks are

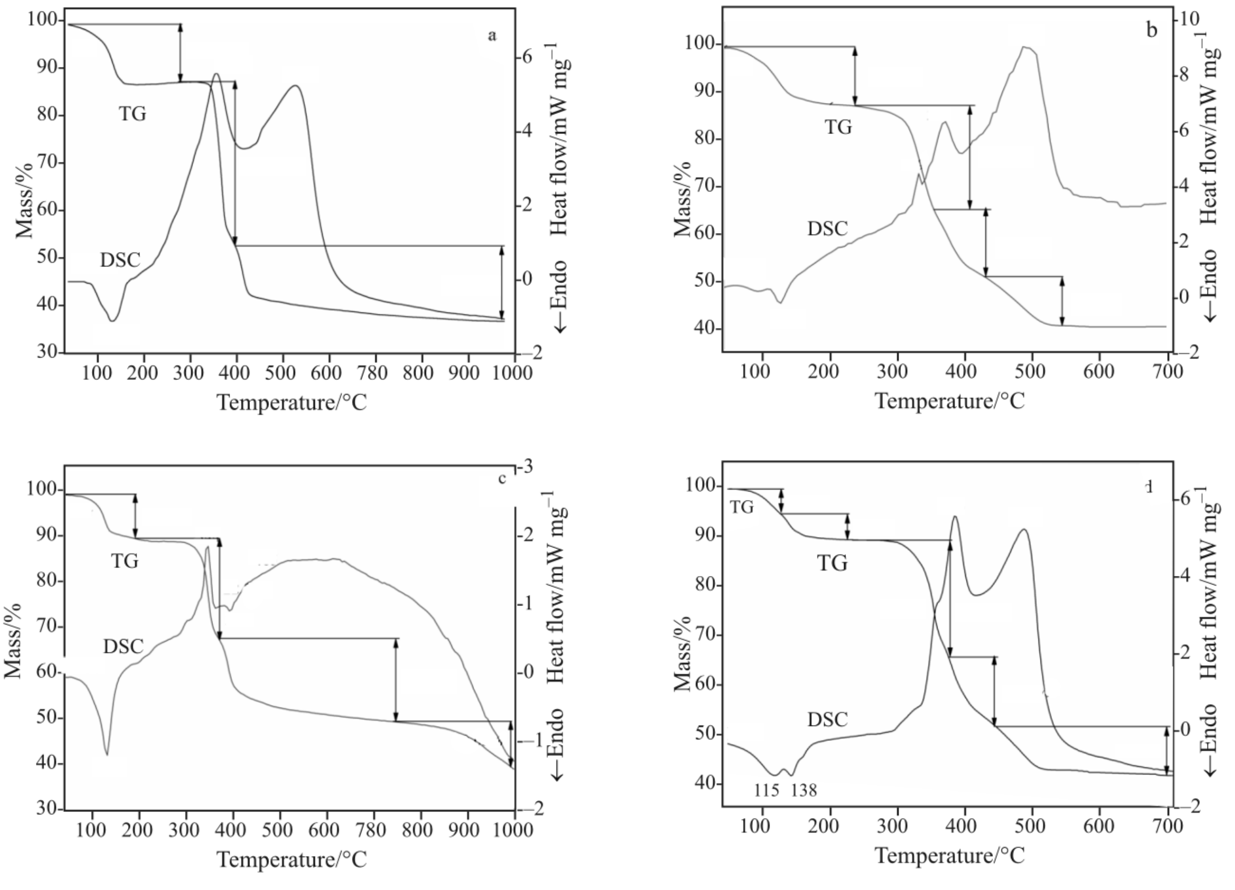

Fig. 4 TG-DSC curves of a – $[Sb_2\text{-}\mu_4\text{-}(EDTA)_2Co(H_2O)_2]\cdot 5.15H_2O$, b – $[Sb_2(EDTA)_2La]NO_3\cdot 8H_2O$, c – $[Sb_2(EDTA)_2Nd]NO_3\cdot 7H_2O$, d – $[Sb_2(EDTA)_2Dy(H_2O)_4]NO_3\cdot 3H_2O$

higher than 3400 cm^{-1} showing that the O atoms of the water molecules are coordinated to the metal ions [12]. The peaks between 3009 and 2948 cm^{-1} can be assigned to the characteristic asymmetric and symmetric stretching vibration from the $-CH_2-$ group [16]. In the infrared spectra of $[Sb_2(EDTA)_2La]NO_3 \cdot 8H_2O$, the absorption peaks at 1585, 1400 and 1384 cm^{-1} may be from the asymmetric and symmetric stretching vibration in the carboxyl groups, respectively. The differences (185 and 200 cm^{-1}) between the frequencies of the absorption peaks confirms that the oxygen atoms of bridge carboxylic groups coordinate with Sb(III) and La(III) ions [13–15]. We can also expect, there must be the corresponding peaks at 714 and 621 cm^{-1} from the different deformation vibration in the carboxyl groups [16]. It is also found that the $\nu_{as(COO)}$ at 1690 cm^{-1} of EDTA red-shifts to 1585 cm^{-1} (non-bridge carboxylic groups) in the complex and $\nu_{s(COO)}$ at 1353 cm^{-1} of EDTA blue-shifts to 1384 cm^{-1} (bridge carboxylic groups) and 1400 cm^{-1} (non-bridge carboxylic groups) in the complex. This indicates that the O atoms of carboxylic groups coordinate with Sb(III) and La(III) ions [13–15]. In the infrared spectrum of $[Sb_2(EDTA)_2Nd]NO_3 \cdot 7H_2O$, the absorption peaks at 1585, 1412 and 1384 cm^{-1} may be from the asymmetric and symmetric stretching vibration in the carboxyl groups, respectively. If this is so, there must be the corresponding peaks at 717 and 615 cm^{-1} from the different deformation vibration in the carboxyl groups [16]. It is also found that the $\nu_{as(COO)}$ at 1690 cm^{-1} of EDTA red-shifts to 1585 cm^{-1} (non-bridge carboxylic groups) in the complex and $\nu_{s(COO)}$ at 1353 cm^{-1} of EDTA blue-shifts to 1384 cm^{-1} (bridge carboxylic groups) and 1412 cm^{-1} (non-bridge carboxylic groups) in the complex. This shows that the O atoms of carboxylic groups must coordinate with Sb(III) and Nd(III) ions [13–15]. In the infrared spctrum of $[Sb_2(EDTA)_2Dy(H_2O)_4] \cdot NO_3 \cdot 3H_2O$, the absorption peaks at 1590, 1414 and 1384 cm^{-1} may be from the asymmetric and symmetric stretching vibration in the carboxyl groups, respectively. Therefore, we can also be expected that there must be the corresponding peaks at 720 and 621 cm^{-1} from the different deformation vibration in the carboxyl groups [16]. It is found that the $\nu_{as(COO)}$ at 1690 cm^{-1} of EDTA red-shifts to 1590 cm^{-1} (non-bridge carboxylic groups) in the complex and $\nu_{s(COO)}$ at 1353 cm^{-1} of EDTA blue-shifts to 1384 cm^{-1} (bridge carboxylic groups) and 1414 cm^{-1} (non-bridge carboxylic groups) in the complex. This confirms that the O atoms of carboxylic groups coordinate with Sb(III) and Dy(III) ions [13–15]. As above mentions, the infrared spectra of the complexes can demonstrate that the Sb(III) ion is coordinated not only by the O atom, but also by the N atom of EDTA. The O atoms of both EDTA and H_2O are coordinated to Ln(III) ion. The two carboxylic O atoms are bidentate as bridge mode connecting the Sb(III) and Ln(III) ion. In the infrared spectra of the Sb–Ln EDTA complexes, the weaker absorption peaks at about 1400 and 1080 cm^{-1} may be from the asymmetric and symmetric stretching vibrations in the NO_3^- group. This indicates that the NO_3^- group is not coordinated to the metallic ions [18]. The absorption peaks at about 1093 and 1040 cm^{-1} may be from various stretching vibrations of the C–N and C–C bond in EDTA, respectively. In the far-infrared region, the frequency of the stretching vibration of the Sb–N and Sb–O bond is about 465 and 370 cm^{-1} respectively [12, 17]. The heavier the atom in the chemical bond is, the lower the vibration frequency of the chemical bond is. Therefore, it may be reasonable to assign the peaks at 350 cm^{-1} to the stretching vibration of Ln–O bond in the complex [17, 18].

The possible pyrolysis reactions, the experimental and calculated percentage mass losses in the thermal decomposition process of the complexes are summarized in Table 2. As Figs 4a and 5a show, the first mass loss of $[Sb_2\text{-}\mu_4\text{-}(EDTA)_2Co(H_2O)_2] \cdot 5.15H_2O$ occurs about 130°C, then, the sample will gradually lose $7.15H_2O$ molecules. This consists with the single crystal structure. The experimental percentage mass loss (13.10%) closes to the calculated one (12.77%). With increasing temperature, two $(CH_2)_2NCH_2COO$ groups will be eliminated from the two ligands (EDTA). In this case, the ligands will become four nitrilotriacetic radicals, $[N(CH_2COO)_3]^{3-}$. Then, the $N(CH_2)_3$ groups are eliminated from $[N(CH_2COO)_3]^{3-}$. The experimental percentage mass loss (32.59%) is close to the calculated one (30.96%). When temperature is over 400°C, the sample will lose the residual CO. The eliminated CO can burn in air and release enormous heat. This is why there is an appreciable exothermic peak at 527.5°C in DSC and DTA curves. Last, the residue of the thermal decomposition may be $CoSb_2O_6$, in which the pyrolysis product is stibial mixed oxide compound because of oxygen atmosphere at high temperature. To check the residue, a certain amount of $[Sb_2\text{-}\mu_4\text{-}(EDTA)_2Co(H_2O)_2] \cdot 5.15H_2O$ is placed in an alumina crucible and heated in a muffle furnace at 1000°C for 4 h. Then, the powder X-ray diffraction pattern of the pyrolysis product is recorded. As the Fig. 2f shows, its characteristic peaks are mostly consistent with the normative peaks according to JCPDS cards No. 18-0403. The pyrolysis product of the complex $[Sb_2\text{-}\mu_4\text{-}(EDTA)_2Co(H_2O)_2] \cdot 5.15H_2O$ is similar to the complex $[CaSb_2(EDTA)_2(H_2O)_8]_n$ which in air above 700°C allows the easy preparation of the mixed

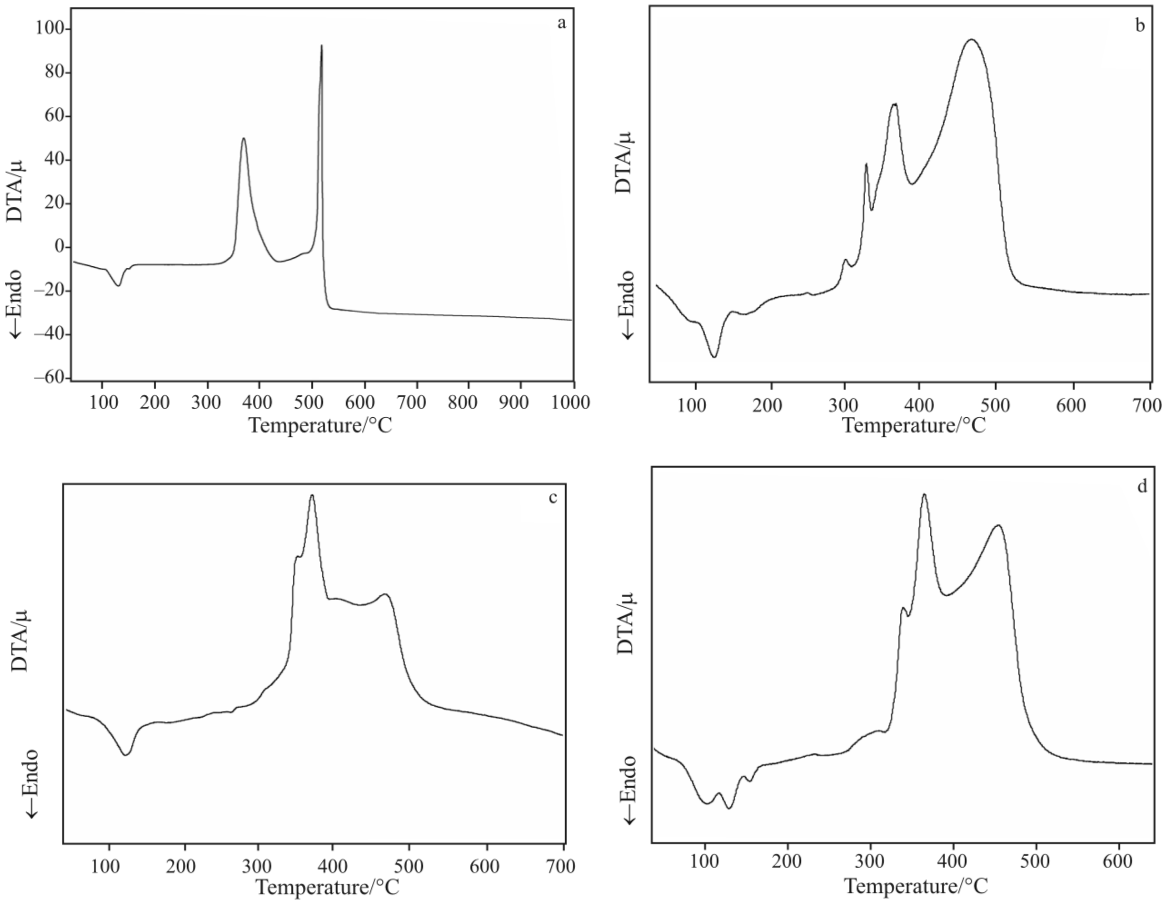

Fig. 5 DTA curves of a – $[Sb_2\text{-}\mu_4\text{-}(EDTA)_2Co(H_2O)_2]\cdot 5.15H_2O$, b – $[Sb_2(EDTA)_2La]NO_3\cdot 8H_2O$, c – $[Sb_2(EDTA)_2Nd]NO_3\cdot 7H_2O$, d – $[Sb_2(EDTA)_2Dy(H_2O)_4]NO_3\cdot 3H_2O$

oxide $CaSb_2O_6$ [19]. Therefore, the pyrolysis product must be $CoSb_2O_6$. As Figs 4b and 5b show, the first mass loss of $[Sb_2(EDTA)_2La]NO_3\cdot 8H_2O$ occurs about 123.6°C, then, the sample will gradually lose sixteen lattice water molecules (based on double $[Sb_2(EDTA)_2La]NO_3\cdot 8H_2O$ molecules). This consists with the results of the elemental analysis. The experimental percentage mass loss (12.99%) very consists with the calculated one (12.37%). With increasing temperature, two NO_3^- and four $(CH_2)_2NCH_2COO$ groups will be eliminated from the ligands (EDTA). In this case, four EDTA will become two $[N(CH_2COO)_3]^{3-}$. The calculated percentage mass loss (22.51%) closes to the experimental one (21.49%). Then, four $N(CH_2)_3$ groups are eliminated from the four $[N(CH_2COO)_3]^{3-}$. Besides, two CO_2 molecules will also be eliminated from the ligands. The experimental percentage mass loss (12.85%) consists with the calculated one (13.41%). Due to the chemical reaction between the pyrolysis products $N(CH_2)_3$ and the oxygen in air, this leads to appearance of an exothermic peak at 368.4°C in DSC and DTA curves. When temperature is over 400°C, the sample will lose the residual CO and O. The eliminated CO can burn in air and release enormous heat. This is also why there is an appreciable exothermic peak at 489.6°C in DSC and DTA curves. At one time, Sb(III) and La(III) will become the oxide of Sb and La. Last, the residue of the thermal decomposition will be the mixture of Sb_2O_3 and La_2O_3. As above mentioned, NO_3^- can very easily be eliminated from the complex. This means that NO_3^- is coordinated neither to the Sb(III) ion nor to the La(III) ion in the complex. As Figs 4c and 5c show, there is an endothermic peak at about 120.7°C in DSC and DTA curves of $[Sb_2(EDTA)_2Nd]NO_3\cdot 7H_2O$. The percentage mass loss shows that the sample contains the fourteen water molecules (based on double $[Sb_2(EDTA)_2Nd]\cdot NO_3\cdot 7H_2O$ molecules). This consists with the results of the elemental analysis. The second mass loss of the sample occurs at about 343.6°C. Two NO_3^- and four $(CH_2)_2NCH_2COO$ groups of the ligands (EDTA) will be eliminated from the sample. In this case, four EDTA will become four $[N(CH_2COO)_3]^{3-}$. The calculated percentage mass loss (22.72%) is very close to the experimental percentage mass loss (22.37%). Then, four $N(CH_2)_3$ groups will be eliminated from the four $[N(CH_2COO)_3]^{3-}$. Besides, six CO will also be eliminated from the ligands. The experimental percentage mass loss (17.57%) consists very well with the calculated one (17.03%). Due to the chemical reaction between the pyrolysis products $N(CH_2)_3$ and the oxygen in air, this will lead to appearance of an exothermic peak at 391.0°C in DSC curve. When temperature is over 400°C, the sample will lose the residual CO and O. The eliminated CO can burn in air and release enormous heat. Figure 5c shows an appreciable exothermic peak at 464.5°C in DTA curve of $[Sb_2(EDTA)_2Nd]NO_3{\cdot}7H_2O$. When temperature is over 400°C, Sb(III) and Nd(III) will become the oxide of Sb and Nd, respectively. Last, the residue of the thermal decomposition of the complex will be the mixture of Sb_2O_3 and Nd_2O_3. As above mentioned, NO_3^- can very easily be eliminated from the complex, which indicates that NO_3^- is not coordinated to metallic ions in the complex. Figures 4d and 5d also show, the mass loss of $[Sb_2(EDTA)_2Dy(H_2O)_4]NO_3{\cdot}3H_2O$ occurs about 114.5 and 138.2°C. Then, the sample will gradually lose six and eight water molecules (based on double $[Sb_2(EDTA)_2Dy(H_2O)_4]NO_3{\cdot}3H_2O$ molecules). This also consists with the results of the elemental analysis. The total experimental percentage mass loss (10.25%) of the sample in the two steps very close to the calculated one (10.78%). With increasing temperature, two NO_3^- and four $(CH_2)_2NCH_2COO$ groups will be eliminated from the ligands (EDTA). At one time, four EDTA become four $[N(CH_2COO)_3]^{3-}$. The calculated percentage mass loss (22.40%) consists very well with the experimental percentage mass loss (22.42%). Then, four $N(CH_2)_3$ groups will be eliminated from four $[N(CH_2COO)_3]^{3-}$. Besides, six CO will also be eliminated from the ligands. The experimental percentage mass loss (16.71%) consists with the calculated one (16.76%). Due to the chemical reaction between the pyrolysis products $N(CH_2)_3$ and the oxygen in air, this leads to appearance of an exothermic peak at 378.5°C in DSC and DTA curves. When temperature is over 400°C, the sample will gradually lose the residual CO and O. The eliminated CO can burn in air and release enormous heat. This is just why there is an appreciable exothermic peak at 479.8°C in DSC and DTA curves. At one time, Sb(III) and Dy(III) become the oxides. Last, the residue of the thermal decomposition of the complex is the mixture of Sb_2O_3 and Dy_2O_3. Similarly, NO_3^- is coordinated neither to the Sb(III) ion nor to the Dy(III) ion in the complex.

Conclusions

Four new EDTA-linked heterometallic complexes of Sb(III) and *M* (*M*=Co(II), La(III), Nd(III), Dy(III)) are synthesized. The formula of the complex is $[Sb_2\text{-}\mu_4\text{-}(EDTA)_2Co(H_2O)_2]{\cdot}5.15H_2O$, $[Sb_2(EDTA)_2La]NO_3{\cdot}8H_2O$, $[Sb_2(EDTA)_2Nd]NO_3{\cdot}7H_2O$ and $[Sb_2(EDTA)_2Dy]NO_3{\cdot}7H_2O$, respectively. There is the μ-bridges of carboxylic groups of EDTA between the Sb(III) and M ions in the complex. The trivalent antimony ion is coordinated to four O atoms and two N atoms of one EDTA. The trivalent lanthanide ion is coordinated to O atoms both from EDTA and water molecule. NO_3^- is not coordinated to the metal ion in the complexes. The thermal analysis demonstrates the complex formation between the Sb(III) ion, M ion and EDTA. The mass loss of the sample and determination of the metal content in the intermediate in test experiment also support the pyrolysis reactions in the thermal decomposition process of the complexes.

Acknowledgements

The authors thank to Science and Technology Bureau of Sichuan Province and Southwest University of Science and Technology researching project (No. 05JY029-113, No. ZK043129).

Supplementary data

Crystallographic data for $[Sb_2\text{-}\mu_4\text{-}(EDTA)_2Co(H_2O)_2]{\cdot}5.15H_2O$ has been deposited with the Cambridge Crystallographic Data Centre. The deposition number is CCDC-637089. The data can be obtained free of charge on application to the Director, CCDC, 12 Union Road, Cambridge, CB2 1EZ, UK, fax: +44 1223 366 033, e-mail: deposit@ccdc.ac.uk or on the web www: http://www.ccdc.cam.ac.uk or from the authors on request.

References

1 V. Stavila, A. Gulea, N. Popa, S. Shova, A. Merbach, Y. A. Simonov and J. Lipkowski, Inorg. Chem. Commun., 7 (2004) 634.

2 N. Sakagami, Y. Yamada, T. Tonno and K. Okamoto, Inorg. Chim. Acta, 288 (1999) 7.

3 D. X. Jia, J. Deng, Q. X. Zhao and Y. Zhang, J. Mol. Struct., 833 (2007) 114.

4 Q. X. Zhao, D. X. Jia, Y. Zhang, L. F. Song and J. Dai, Inorg. Chim. Acta, 360 (2007) 1895.

5 T. Yi, S. Gao and B. G. Li, Polyhedron, 17 (1998) 2243.

6 V. Lecureur, D. Lagadic-Gossmann and O. Fardel, Int. J. Oncol., 20 (2002) 1071.

7 W. X. Zhang, S. Y. Liu, C. Q. Ma and D. H. Jiang, Thermochim. Acta, 376 (2001) 163.

8 W. Yan, C. Ma, J. Wu, W. Zhang and D. Jang, J. Therm. Anal. Cal., 58 (1999) 393.

9 S. Durmuş, Ü. Ergun, J. C. Jaud, K. C. Emregül, H. Fuess and O. Atakol, J. Therm. Anal. Cal., 86 (2006) 337.

10 G. M. Sheldrick, SHELXS-97, Program for X-ray Crystal Structure Solution, University of Göttingen, Germany, 1990.

11 G. M. Sheldrick, SHELXS-97, Program for X-ray Crystal Structure Solution, University of Göttingen, Germany, 1997.

12 K. Nakamoto, Infrared and Raman Spectra of Inorganic and Coordination Compounds, 4th Ed., John Wiley & Sons Inc., 1986.

13 R. Y. Wang, J. R. Li, T. Z. Jin, G. X. Xu, Z. Y. Zhou and X. G. Zhou, Polyhedron, 16 (1997) 2037.

14 R. Y. Wang, J. R. Li, T. Z. Jin and G. X. Xu, Polyhedron, 16 (1997) 1361.

15 J. Wang, X. D. Zhang, Z. R. Liu and W. G. Jia, J. Mol. Struct., 613 (2002) 189.

16 K. Nakanshi and P. H. Solomon, Infrared Absorption Spectroscopy, 2nd Ed., Holden-Day, San Francisco 1974.

17 Y. C. Guo, S. R. Luan, Y. R. Chen, X. S. Zang, Y. Q. Jia, G. Q. Zhong and S. K. Ruan, J. Therm. Anal. Cal., 68 (2002) 1025.

18 M. D. Jin and W. X. Zhu, The Research Methods of the Coordination Chemistry, 1st Ed, Science Press, Chinese 1996.

19 B. Marrot, C. Brouca-Cabarrecq and A. Mosset, J. Chem. Crystallogr., 28 (1998) 447.

Received: May 30, 2007
Accepted: November 6, 2007

DOI: 10.1007/s10973-007-8579-5